Electronic Supplementary Information

Oxidative *versus* Basic Asynchronous Hydrogen Atom Transfer Reactions of Mn(III)-Hydroxo and Mn(III)-Aqua Complexes

Jisheng Zhang,[a] Yong-Min Lee,[a] Mi Sook Seo,[a] Youngsuk Kim,[c] Eunsung Lee,[c] Shunichi Fukuzumi*[ab] and Wonwoo Nam*[a]

[a] Department of Chemistry and Nano Science, Ewha Womans University, Seoul 03760, Korea

[b] Faculty of Science and Engineering, Meijo University, Nagoya, Aichi 468-8502, Japan

[c] Department of Chemistry, Pohang University of Science and Technology, Pohang 37673, Korea

*E-mail: wwnam@ewha.ac.kr, fukuzumi@chem.eng.osaka-u.ac.jp

Table of Contents

Table S1 Crystallographic data and refinements for $[(dpaq^{5R})Mn^{III}(OH)]^{+}$ (R = NO_2, Me, and OMe)

	$[(dpaq^{5NO2})Mn^{III}(OH)](OTf)$	$[(dpaq^{5Me})Mn^{III}(OH)](OTf)$ [a]	$[(dpaq^{5OMe})Mn^{III}(OH)](OTf)$
empirical formula	$C_{24}H_{20}F_3MnN_6O_7S$	$C_{27}H_{26}F_3MnN_6O_5S$	$C_{25}H_{23}F_3MnN_5O_6S$
formula weight	648.46	658.54	633.48
temperature (K)	150 K	150 K	150 K
Wavelength (Å)	0.71073	0.71073	0.71073
crystal system	monoclinic	monoclinic	monoclinic
space group	$P2_1/n$	$P2_1/n$	$P2_1/c$
unit cell dimensions			
a (Å)	8.8110(17)	9.1663(6)	12.8436(9)
b (Å)	22.663(4)	24.9767(17)	13.4456(9)
c (Å)	13.337(3)	12.4192(9)	15.6922(10)
α (°)	90	90	90
β (°)	100.823(10)	96.255(3)	107.733(3)
γ (°)	90	90	90
volume ($Å^{-3}$)	2615.8(9)	2826.4(3)	2581.1(3)
Z	4	4	4
calculated density (g/cm^{-3})	1.647	1.548	1.630
absorption coefficient (mm^{-1})	0.664	0.610	0.667
reflections collected	49120	53032	95609
absorption correction	multi-scan (T_{min} = 0.920, T_{max} = 0.970)	multi-scan (T_{min} = 0.880, T_{max} = 0.970)	multi-scan (T_{min} = 0.900, T_{max} = 0.980)
independent reflections	6508	7031	6697
goodness-of-fit on F^2	0.998	1.079	1.034
R [F^2>2sigma(F^2)]	0.0370	0.0260	0.0374
wR^2	0.1318	0.0673	0.0864

[a] Actual formula of this crystal structure is included an CH_3CN solvent molecule.

Table S2 Selected bond distances (Å) and angles (º) for $[(dpaq^{5R})Mn^{III}(OH)]^{+}$

	$[(dpaq^{5NO2})Mn^{III}(OH)]^{+}$	$[(dpaq^{5Me})Mn^{III}(OH)]^{+}$	$[(dpaq^{5OMe})Mn^{III}(OH)]^{+}$
bond distance (Å)			
Mn1-N4	1.9739(15)	1.9703(9)	1.9831(16)
Mn1-O1	1.8081(15)	1.8073(9)	1.8038(14)
Mn1-N5	2.0592(15)	2.0592(10)	2.0774(17)
Mn1-N2	2.1685(17)	2.1580(10)	2.1901(16)
Mn1-N1	2.1937(17)	2.2256(10)	2.2033(17)
Mn1-N3	2.2284(17)	2.2458(10)	2.2116(16)
bond angle (°)			
O1-Mn1-N4	174.46(6)	178.4(4)	178.54(7)
O1-Mn1-N5	94.81(6)	98.72(4)	99.12(7)
N4-Mn1-N5	79.79(6)	79.76(4)	80.05(6)
O1-Mn1-N2	102.78(6)	98.65(4)	99.09(7)
N4-Mn1-N2	82.59(6)	82.89(4)	81.72(6)
N5-Mn1-N2	162.36(6)	162.57(4)	161.73(6)
O1-Mn1-N1	91.73(7)	88.16(4)	93.92(7)
N4-Mn1-N1	88.21(6)	92.67(4)	87.44(6)
N5-Mn1-N1	102.14(6)	102.86(4)	102.27(6)
N2-Mn1-N1	76.39(6)	76.18(4)	77.98(6)
O1-Mn1-N3	95.97(7)	94.75(4)	87.00(6)
N4-Mn1-N3	86.52(6)	85.12(4)	92.03(6)
N5-Mn1-N3	102.85(6)	103.00(4)	103.50(6)
N2-Mn1-N4	76.77(6)	77.05(4)	75.96(6)
N1-Mn1-N3	153.09(6)	153.21(4)	153.73(6)

Table S3 Second-order rate constants (k_2) for the oxidation of 4-MeO-2,6-^{t}Bu$_2$C$_6$H$_2$OH by [(dpaq^{5R})Mn^{III}(OH)]$^+$ (R = NO_2, Cl, H, Me, and OMe) under an Ar atmosphere in MeCN/H_2O (98:2 v/v) at 298 K

R	k_2, M^{-1} s^{-1}
NO_2	4.2(3)
Cl	2.3(2)
H	1.7(1)
Me	1.6(1)
OMe	1.5(1)

Table S4 Second-order rate constants (k_{et}) for the electron transfer from $Me_{10}Fc$ to $[(dpaq^{5R})Mn^{III}(OH)]^+$ (R = NO_2, Cl, H, Me, and OMe) under an Ar atmosphere in $MeCN/H_2O$ (98:2 v/v) at 298 K

R	k_{et}, M^{-1} s^{-1}
NO_2	95(8)
Cl	30(3)
H	14(1)
Me	11(1)
OMe	7.1(6)

Table S5 Crystallographic data and refinements for $[(dpaq^{5Me})Mn^{III}(OH_2)]^{2+}$

	$[(dpaq^{5Me})Mn^{III}(OH_2)](OTf)_2$ [a]
empirical formula	$C_{52}H_{48}F_{12}Mn_2N_{10}O_{16}S_4$
formula weight	1535.12
temperature (K)	100
wavelength (Å)	0.7000
crystal system	triclinic
space group	*P*-1
unit cell dimensions	
a (Å)	10.012(2)
b (Å)	15.900(3)
c (Å)	19.840(4)
α (°)	88.44(3)
β (°)	77.95(3)
γ (°)	89.88(3)
volume (Å ^{3})	3087.6(11)
Z	2
calculated density (g/cm^{-3})	1.652
absorption coefficient (mm^{-1})	0.647
reflections collected	41817
absorption correction	-
independent reflections	11486
goodness-of-fit on F^2	1.063
R [F^2 > 2sigma(F^2)]	0.1067
wR^2	0.2567

[a] Refinement details for $[(dpaq^{5Me})Mn^{III}(OH_2)](OTf)_2$:

1. Twinned data refinement[S1] Scales: 0.696(3) 0.304(3)

2. Fixed U_{iso}

At 1.2 times of: All C(H) groups, All C(H,H) groups

At 1.5 times of: All C(H,H,H) groups, All O(H,H) groups

3.a Rotating group: O31(H31A,H31B), O62(H62A,H62B)

3.b Secondary CH2 refined with riding coordinates:

C15(H15A,H15B), C17(H17A,H17B), C24(H24A,H24B), C46(H46A,H46B), C48(H48A,H48B), C56(H56A,H56B)

3.c Aromatic/amide H refined with riding coordinates:

C2(H2), C3(H3), C4(H4), C8(H8), C9(H9), C19(H19), C20(H20), C21(H21),C22(H22), C26(H26), C27(H27), C28(H28), C29(H29), C33(H33), C34(H34), C38(H38), C39(H39), C40(H40), C50(H50), C51(H51), C52(H52), C53(H53), C57(H57), C58(H58), C59(H59), C60(H60)

3.d Idealized Me refined as rotating group:

C7(H7A,H7B,H7C), C36(H36A,H36B,H36C)

(S1) A. L. Spek, Structure Validation in Chemical Crystallography, *Acta Cryst*., 2009, **D65**, 148-155.

Table S6 Selected bond distances (Å) and angles (º) for $[(dpaq^{5Me})Mn^{III}(OH_2)]^{2+}$

	$[(dpaq^{5Me})Mn^{III}(OH_2)]^{2+}$
bond distance (Å)	
Mn1-N4	1.939(5)
Mn1-O1	1.961(4)
Mn1-N5	2.018(5)
Mn1-N2	2,121(5)
Mn1-N1	2.226(6)
Mn1-N3	2.247(6)
bond angle (°)	
O1-Mn1-N4	178.0(2)
O1-Mn1-N5	97.57(19)
N4-Mn1-N5	81.1(2)
O1-Mn1-N2	98.12(19)
N4-Mn1-N2	83.2(2)
N5-Mn1-N2	164.2(2)
O1-Mn1-N1	90.7(2)
N4-Mn1-N1	91.1(2)
N5-Mn1-N1	100.0(2)
N2-Mn1-N1	78.1(2)
O1-Mn1-N3	88.6(2)
N4-Mn1-N3	90.3(2)
N5-Mn1-N3	104.0(2)
N2-Mn1-N4	78.1(2)
N1-Mn1-N3	155.89(19)

Table S7 Second-order rate constants (k_2) for the oxidation of 4-MeO-2,6-^{t}Bu$_2$C$_6$H$_2$OH by $[(dpaq^{5R})Mn^{III}(OH_2)]^{2+}$ (R = NO_2, Cl, H, Me, and OMe) in MeCN at 298 K

R	k_2, M^{-1} s^{-1}
NO_2	3.4(2) × 10
Cl	1.1(1) × 10^3
H	1.6(1) × 10^2
Me	2.1(1) × 10^2
OMe	4.5(3) × 10^3

Table S8 Second-order rate constants (k_2) for the oxidation of 2,4-di-*tert*-butylphenol by $[(dpaq^{5R})Mn^{III}(OH_2)]^{2+}$ (R = NO_2, Cl, H, Me, and OMe) in MeCN at 298 K

R	k_2, M^{-1} s^{-1}
NO_2	$2.1(1) \times 10^{-1}$
Cl	2.0(1)
H	1.8(1)
Me	2.0(1)
OMe	$3.0(2) \times 10^{2}$

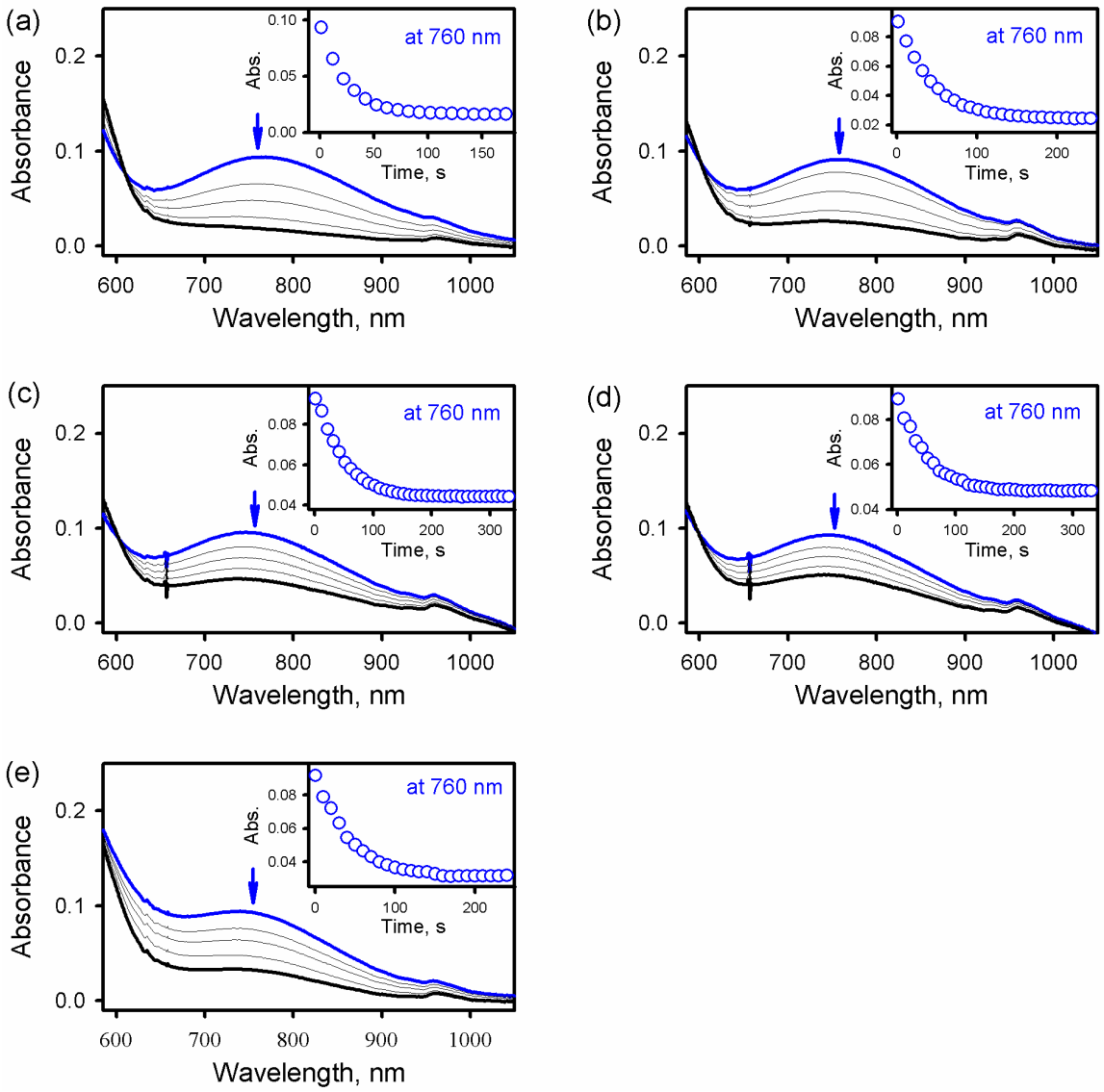

Fig. S1 Visible absorption changes observed in the oxidation of 4-MeO-2,6-$^{t}Bu_2C_6H_2OH$ (10 mM) by $[(dpaq^{5R})Mn^{III}(OH)]^+$ [1.0 mM; R = (a) NO_2, (b) Cl, (c) H, (d) Me, and (e) OMe] under an Ar atmosphere in $MeCN/H_2O$ (98:2 v/v) at 298 K. Insets show the decay time courses of absorbance at 760 nm due to $[(dpaq^{5R})Mn^{III}(OH)]^+$.

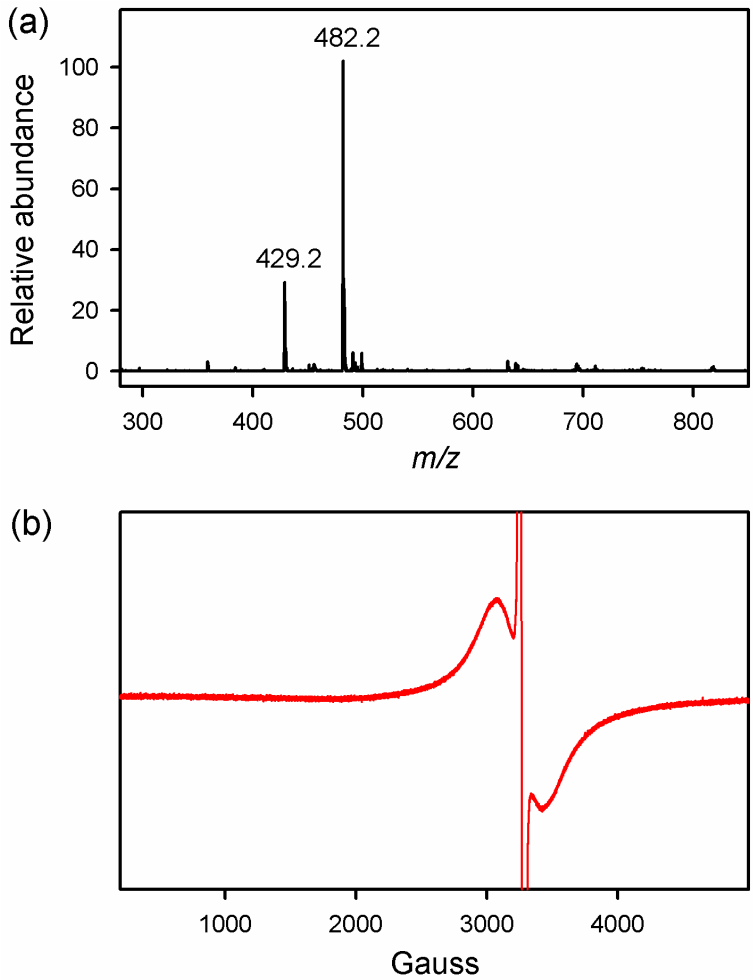

Fig. S2 (a) ESI-MS spectrum of the complete reaction solution obtained in the oxidation of 4-MeO-2,6-$^{t}Bu_2C_6H_2OH$ by $[(dpaq^{5NO2})Mn^{III}(OH)]^+$ under an Ar atmosphere in $MeCN/H_2O$ (98:2 v/v) at 298 K. Peaks at *m/z* = 482.2 and 429.2 correspond to $[(dpaq^{5NO2})Mn^{II}]^+$ (*calc. m/z* = 482.1) and $[dpaq^{5NO2} + 2H^+]^+$ (*calc. m/z* = 429.2), respectively. (b) EPR spectrum of the complete reaction solution obtained in the oxidation of 4-MeO-2,6-$^{t}Bu_2C_6H_2OH$ by $[(dpaq^{5NO2})Mn^{III}(OH)]^+$ under an Ar atmosphere in $MeCN/H_2O$ (98:2 v/v) at 298 K. Spectrum was measured at 77 K. Spectrum shows the signals of Mn(II) species together with phenoxyl radical (i.e., 4-MeO-2,6-$^{t}Bu_2C_6H_2O^{\bullet}$).

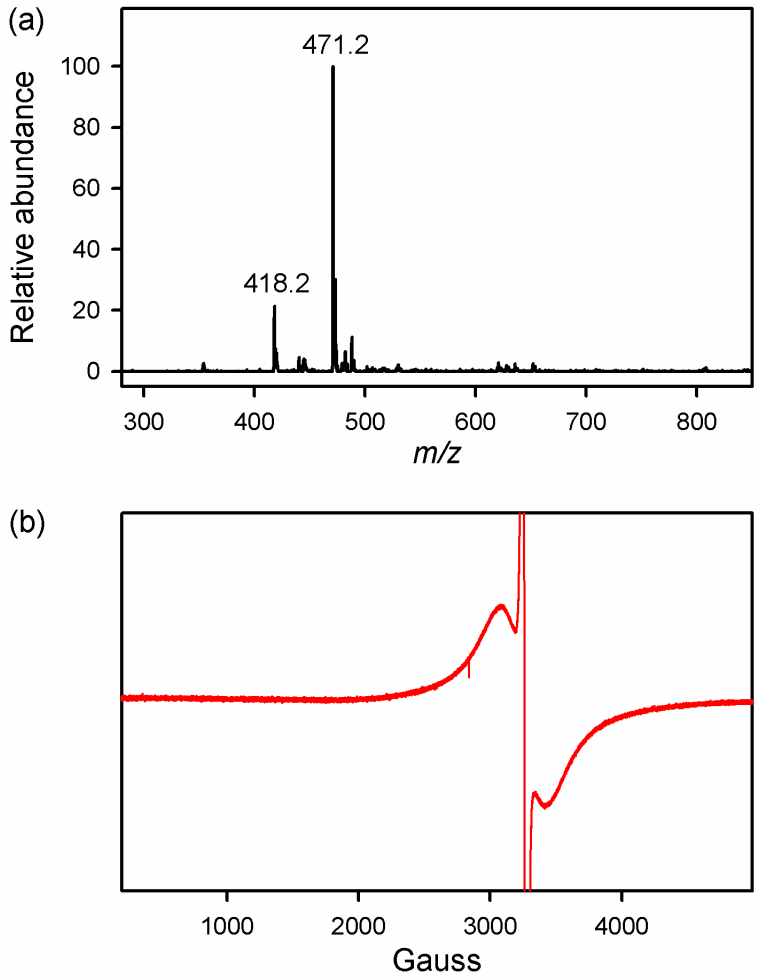

Fig. S3 (a) ESI-MS spectrum of the complete reaction solution obtained in the oxidation of 4-MeO-2,6-$^{t}Bu_2C_6H_2OH$ by $[(dpaq^{5Cl})Mn^{III}(OH)]^+$ under an Ar atmosphere in $MeCN/H_2O$ (98:2 v/v) at 298 K. Peaks at *m/z* = 471.2 and 418.2 correspond to $[(dpaq^{5Cl})Mn^{II}]^+$ (*calc. m/z* = 471.1) and $[dpaq^{5Cl} + 2H^+]^+$ (*calc. m/z* = 418.1), respectively. (b) EPR spectrum of the complete reaction solution obtained in the oxidation of 4-MeO-2,6-$^{t}Bu_2C_6H_2OH$ by $[(dpaq^{5Cl})Mn^{III}(OH)]^+$ under an Ar atmosphere in $MeCN/H_2O$ (98:2 v/v) at 298 K. Spectrum was measured at 77 K. Spectrum shows the signals of Mn(II) species together with phenoxyl radical (i.e., 4-MeO-2,6-$^{t}Bu_2C_6H_2O^{\bullet}$).

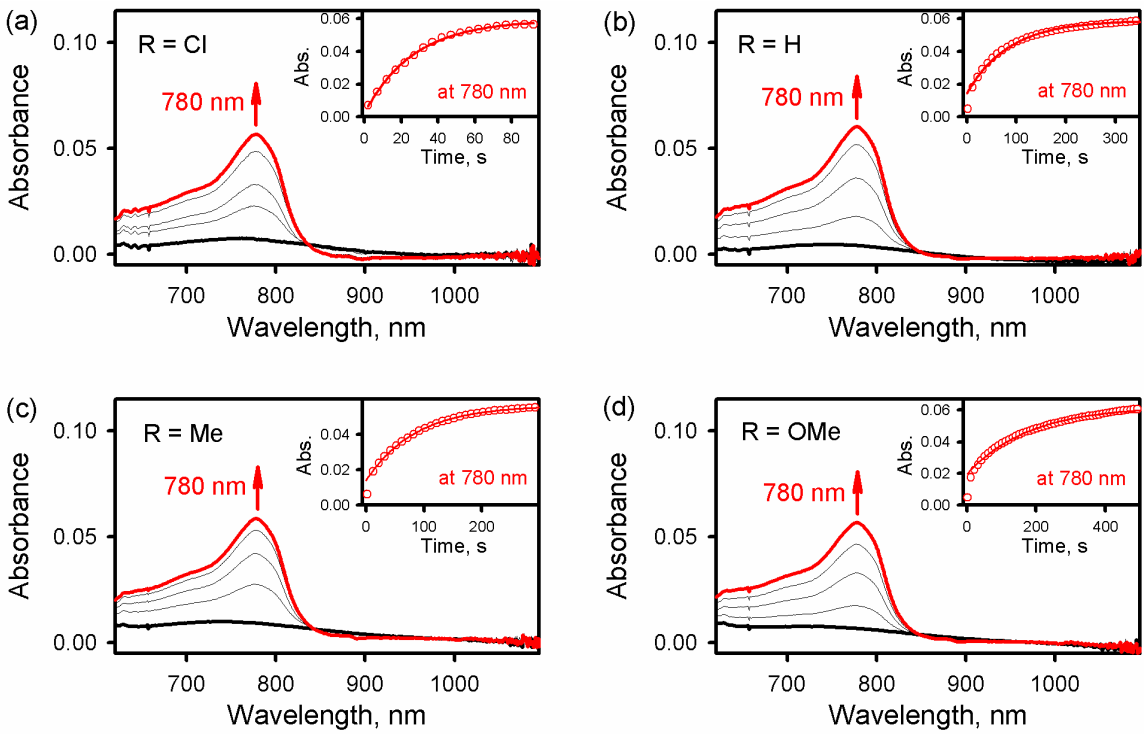

Fig. S4 Visible absorption spectral changes observed in electron transfer from $Me_{10}Fc$ (1.0 mM) to $[(dpaq^{5R})Mn^{III}(OH)]^{+}$ [0.10 mM; R = (a) Cl, (b) H, (c) Me, and (d) OMe] under an Ar atmosphere in $MeCN/H_2O$ (98:2 v/v) at 298 K. Insets show the time courses of absorbance at 780 nm due to the formation of $Me_{10}Fc^{+}$.

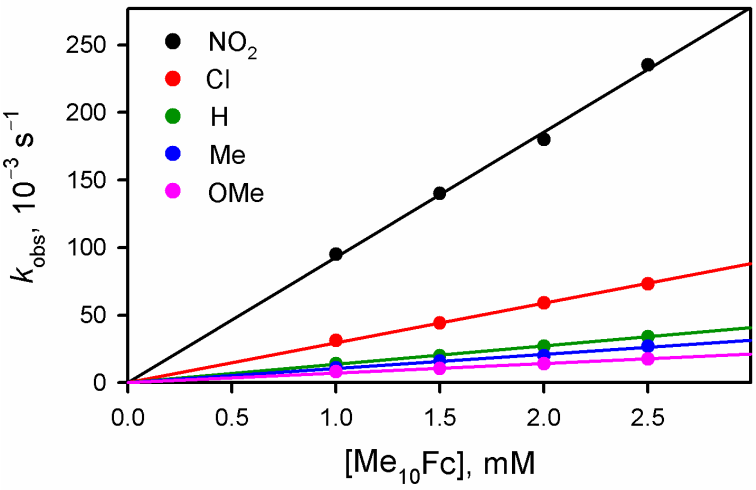

Fig. S5 Plots of pseudo-first-order rate constants (k_{obs}) *vs*. concentration of $Me_{10}Fc$ for the electron transfer from $Me_{10}Fc$ to $[(dpaq^{5R})Mn^{III}(OH)]^{+}$ (0.10 mM; R = NO_2, Cl, H, Me, and OMe) under an Ar atmosphere in $MeCN/H_2O$ (98:2 v/v) at 298 K.

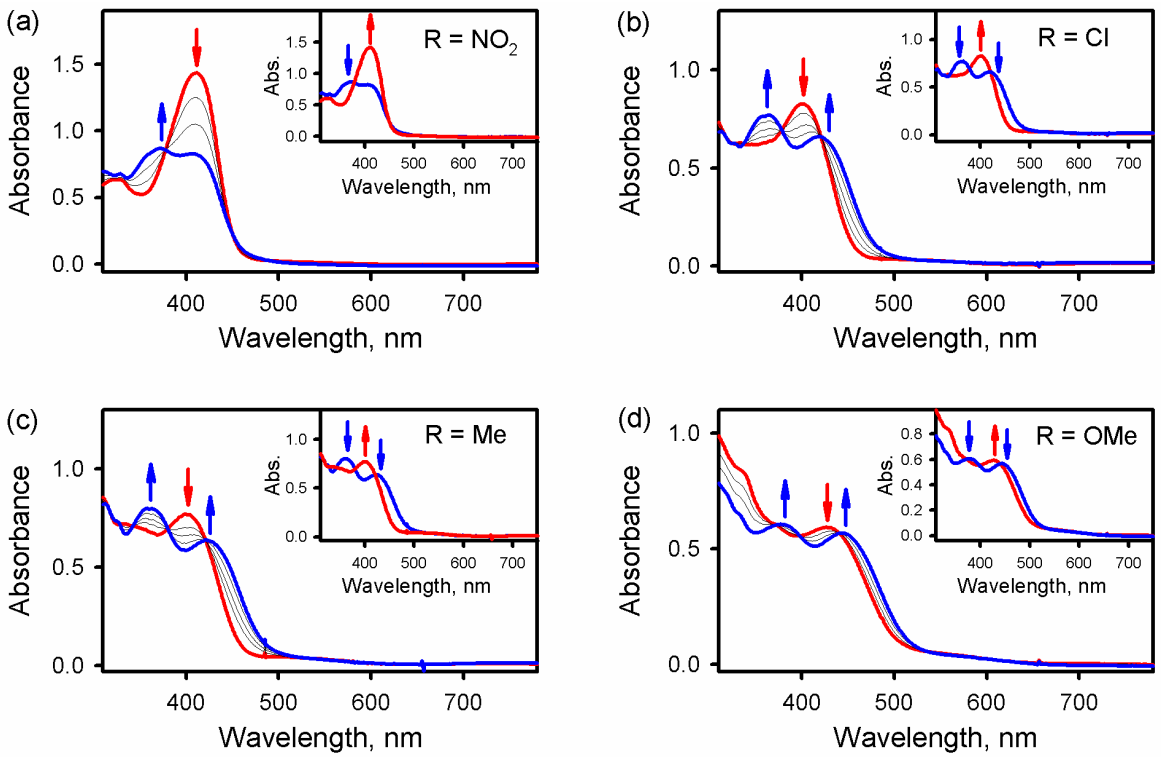

Fig. S6 UV-vis spectral changes for the formation of $[(dpaq^{5R})Mn^{III}(OH_2)]^{2+}$ [blue line; R = (a) NO_2, (b) Cl, (c) Me, and (d) OMe] upon addition of HOTf (1.0 equiv.) to an MeCN solution of $[(dpaq^{5R})Mn^{III}(OH)]^{+}$ (0.10 mM for R = NO_2 and 0.20 mM for R = Cl, Me, and OMe) at 298 K for R = NO_2, Cl and Me and 253 K for OMe. Insets show that all $[(dpaq^{5R})Mn^{III}(OH_2)]^{2+}$ (blue line) was returned back to $[(dpaq^{5R})Mn^{III}(OH)]^{+}$ (red line) upon addition of triethylamine (1.0 equiv.) to $[(dpaq^{5R})Mn^{III}(OH_2)]^{2+}$ in MeCN at 298 K for R = NO_2, Cl, and Me and 253 K for OMe.

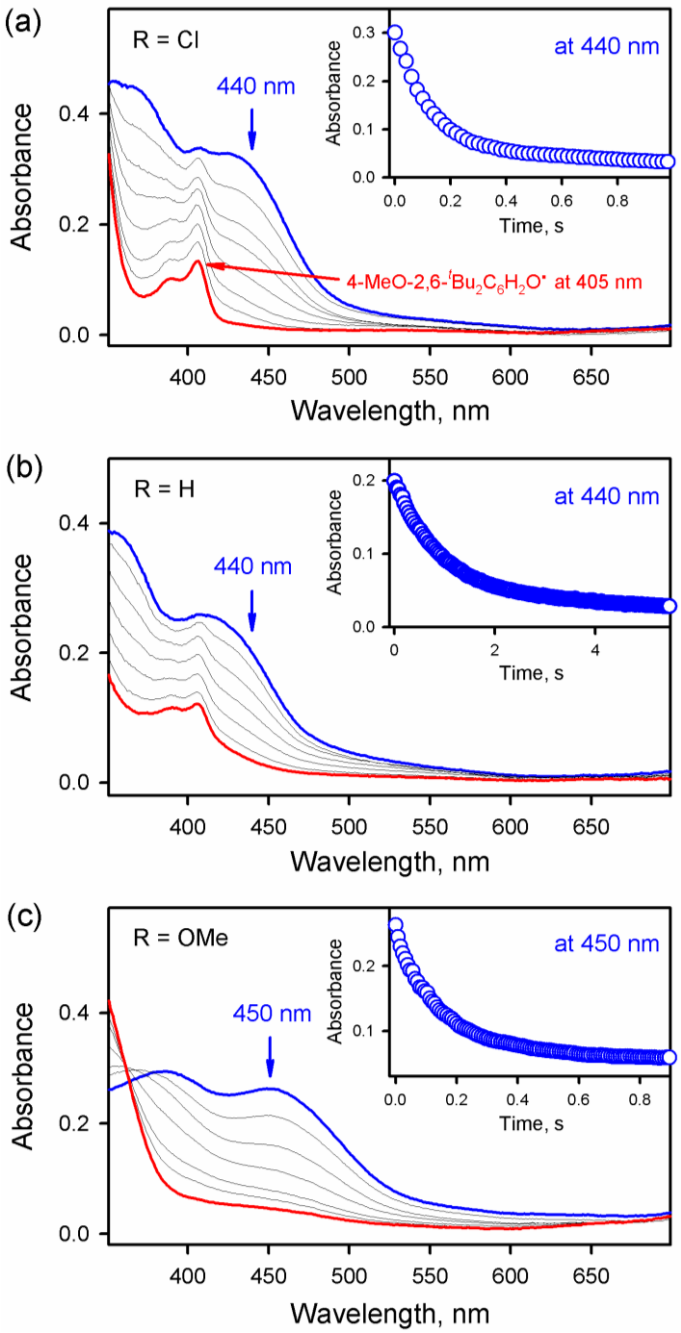

Fig. S7 Visible spectral changes observed in the oxidation of 4-MeO-2,6-$^{t}Bu_2C_6H_2OH$ [(a, b) 6.0 mM and (c) 1.5 mM] by $[(dpaq^{5R})Mn^{III}(OH_2)]^{2+}$ [0.10 mM; R = (a) Cl, (b) H, and (c) OMe] in MeCN at 298 K. Insets show the decay time courses of absorbance at 440 nm (a, b) and 450 nm (c) due to $[(dpaq^{5R})Mn^{III}(OH_2)]^{2+}$.

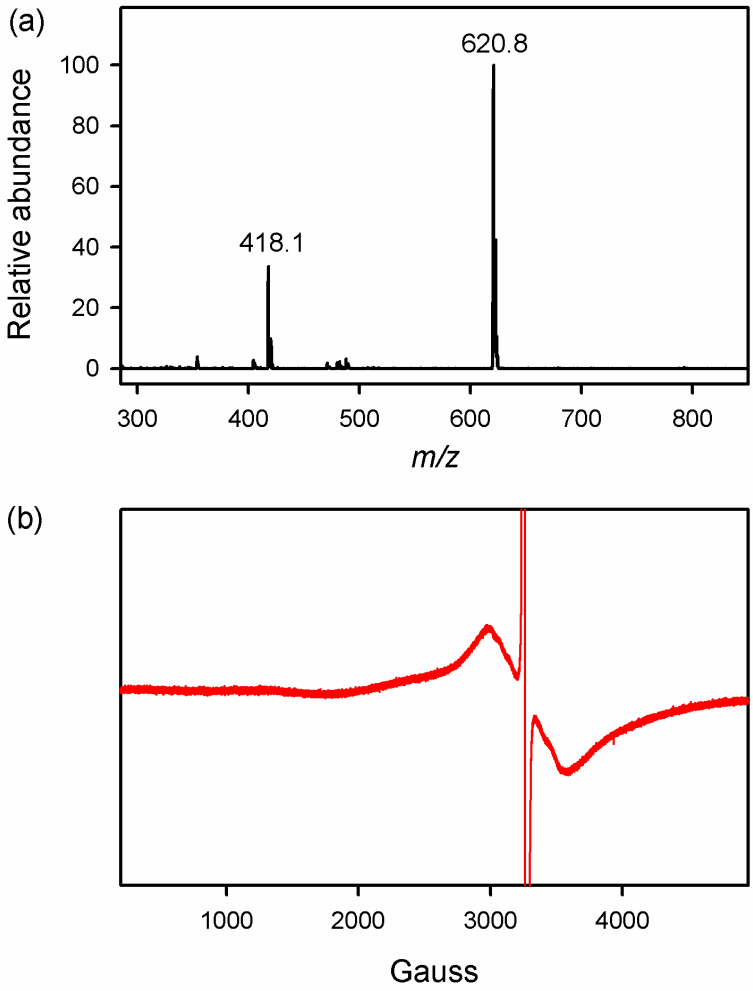

Fig. S8 (a) ESI-MS spectrum of the complete reaction solution obtained in the oxidation of 4-MeO-2,6-$^{t}Bu_2C_6H_2OH$ by $[(dpaq^{5Cl})Mn^{III}(OH_2)]^{2+}$ under an Ar atmosphere in MeCN at 298 K. Peaks at *m/z* = 418.1 and 620.8 correspond to $[dpaq^{5Cl} + 2H^+]^+$ (*calc. m/z* = 418.1) and $[(dpaq^{5Cl})Mn^{II}(HOTf)]^+$ (*calc. m/z* = 621.0), respectively. (b) EPR spectrum of the complete reaction solution obtained in the oxidation of 4-MeO-2,6-$^{t}Bu_2C_6H_2OH$ by $[(dpaq^{5Cl})Mn^{III}(OH_2)]^{2+}$ under an Ar atmosphere in MeCN at 298 K. Spectrum was measured at 77 K. Spectrum shows the signals of Mn(II) species together with phenoxyl radical (i.e., 4-MeO-2,6-$^{t}Bu_2C_6H_2O^{\bullet}$).

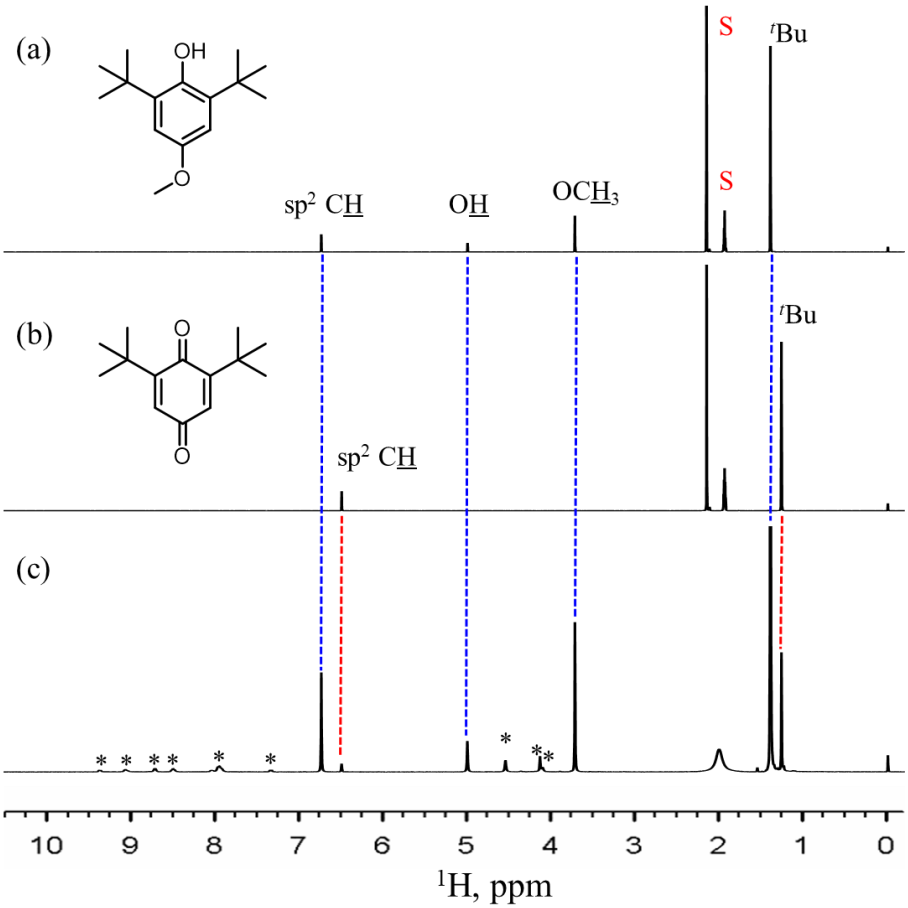

Fig. S9 ^{1}H NMR spectra of the authentic references, (a) 4-MeO-2,6-^{t}Bu$_2$C$_6$H$_2$OH and (b) 2,6-di-*tert*-butyl-1,4-benzoquinone, and (c) the complete reaction solution, which was obtained in the oxidation of 4-MeO-2,6-^{t}Bu$_2$C$_6$H$_2$OH (20 mM) by [(dpaq^{5OMe})Mn^{III}(OH$_2$)]$^{2+}$ (4.0 mM) in CD$_3$CN at 298 K. Spectra were recorded in CD$_3$CN at 298 K. The peaks marked with * and S were originated from the dpaq^{5OMe} ligand and solvent, respectively.

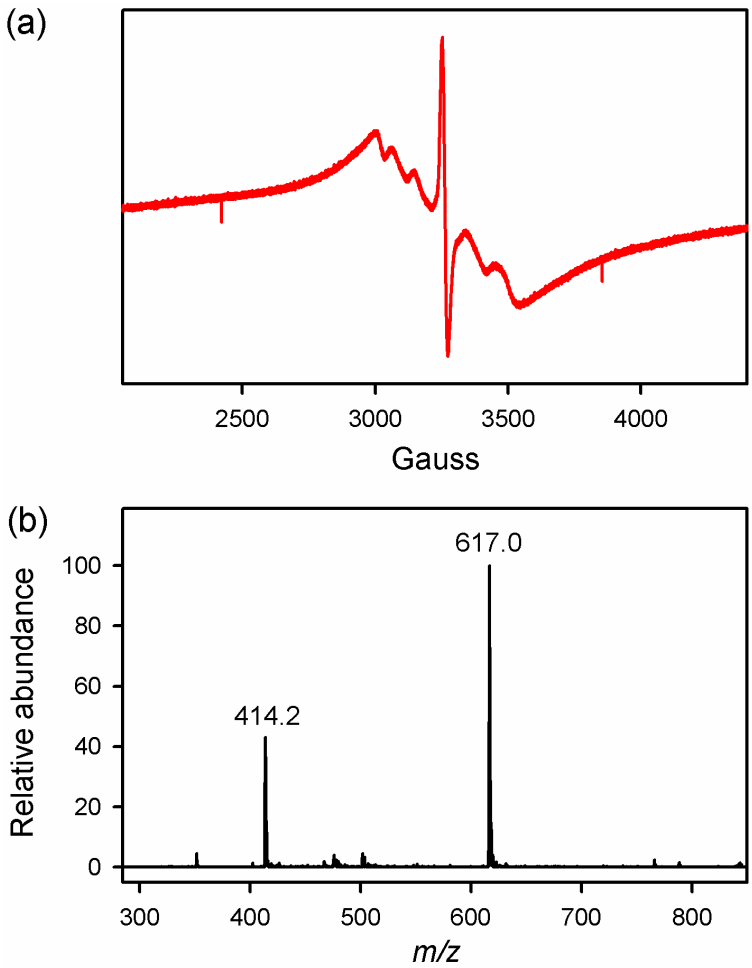

Fig. S10 (a) EPR spectrum of the complete reaction solution obtained in the oxidation of 4-MeO-2,6-$^{t}Bu_2C_6H_2OH$ by $[(dpaq^{5OMe})Mn^{III}(OH_2)]^{2+}$ under an Ar atmosphere in MeCN at 298 K. Spectrum was measured at 77 K. Spectrum shows the signals of Mn(II) species together with phenoxyl radical (i.e., 4-MeO-2,6-$^{t}Bu_2C_6H_2O^{\bullet}$). (b) ESI-MS spectrum of the complete reaction solution obtained in the oxidation of 4-MeO-2,6-$^{t}Bu_2C_6H_2OH$ by $[(dpaq^{5OMe})Mn^{III}(OH_2)]^{2+}$ under an Ar atmosphere in MeCN at 298 K. Peaks at *m/z* = 414.2 and 617.0 correspond to $[dpaq^{5OMe} + 2H^{+}]^{+}$ (*calc. m/z* = 414.2) and $[(dpaq^{5OMe})Mn^{II}(HOTf)]^{+}$ (*calc. m/z* = 617.1), respectively.

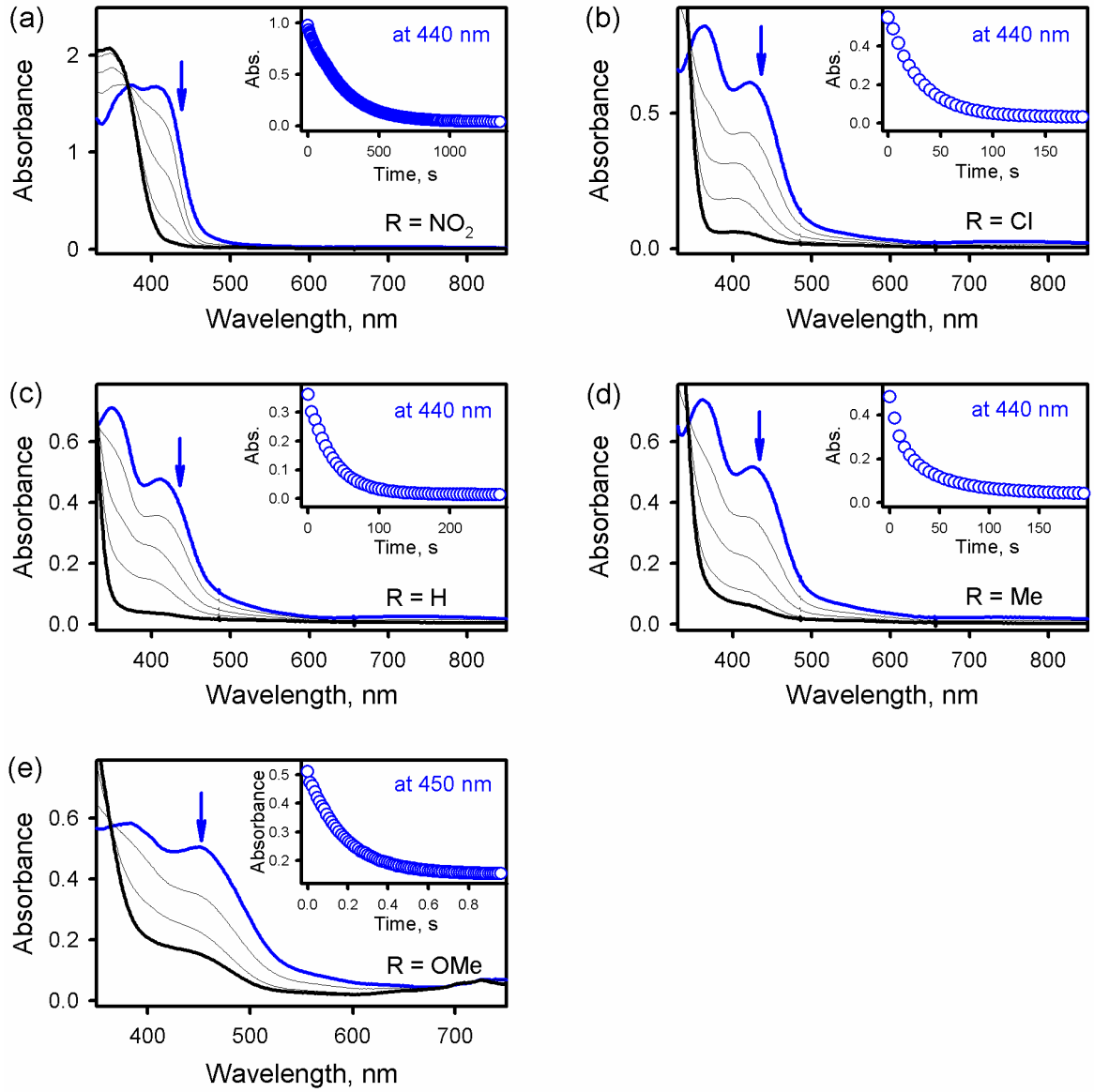

Fig. S11 (a – d) UV-vis spectral changes observed in the oxidation of 2,4-di-*tert*-butylphenol (20 mM) by $[(dpaq^{5R})Mn^{III}(OH_2)]^{2+}$ [0.20 mM; R = (a) NO_2, (b) Cl, (c) H, and (d) Me] in MeCN at 298 K. Insets show the decay time courses of absorbance at 440 nm due to $[(dpaq^{5R})Mn^{III}(OH_2)]^{2+}$. (e) Stopped-flow spectral changes observed in the oxidation of 2,4-di-*tert*-butylphenol (20 mM) by $[(dpaq^{5OMe})Mn^{III}(OH_2)]^{2+}$ (0.20 mM) in MeCN at 298 K. Inset shows the decay time course of absorbance at 450 nm due to $[(dpaq^{5OMe})Mn^{III}(OH_2)]^{2+}$.

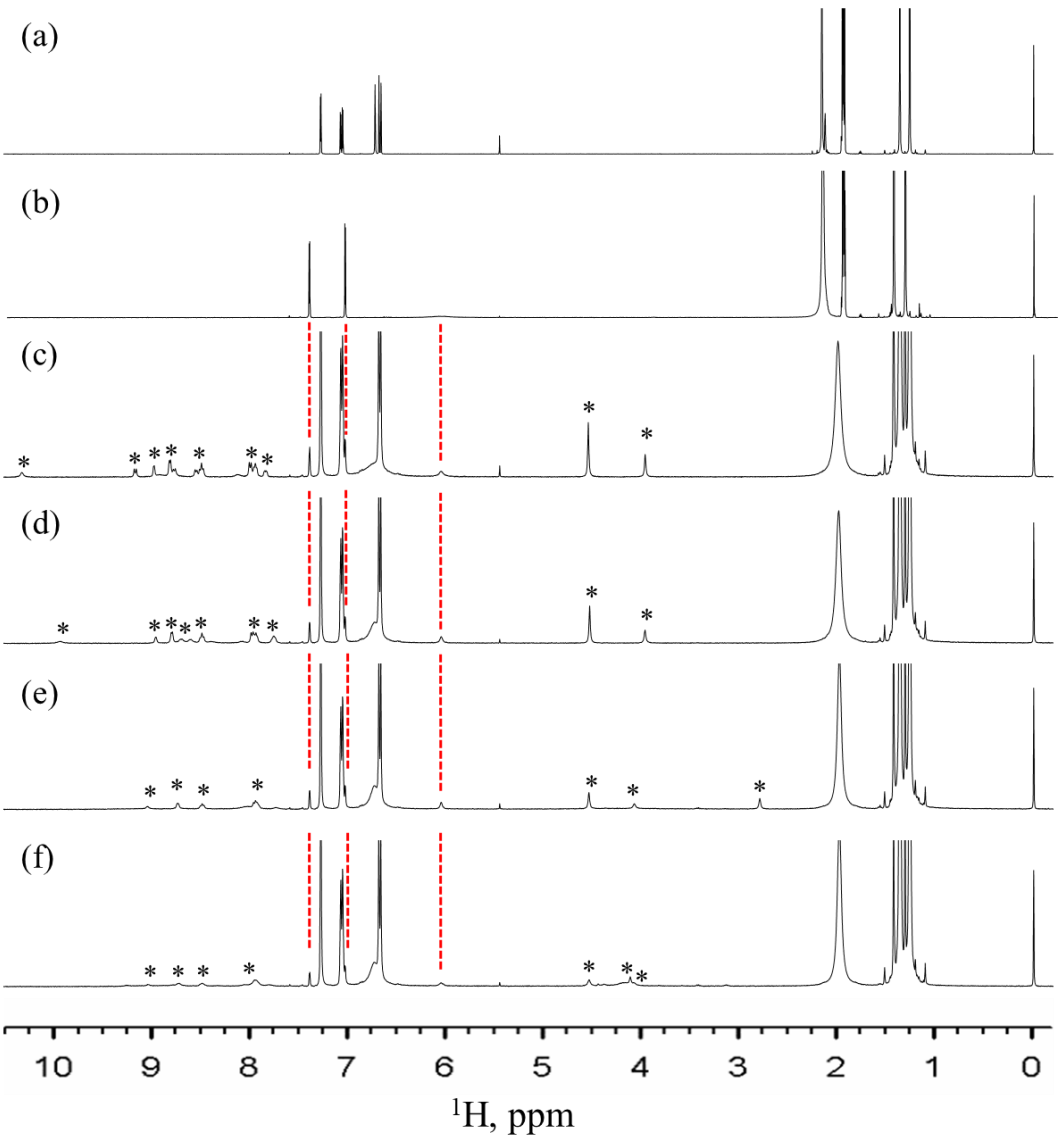

Fig. S12 ^{1}H NMR spectra of the authentic references, (a) 2,4-di-*tert*-butylphenol and (b) 3,3´,5,5´-tetra-*tert*-butylbiphenyl-2,2´-diol, and (c – f) the complete reaction solutions, which were obtained in the oxidation of 2,4-di-*tert*-butylphenol (40 mM) by $[(dpaq^{5R})Mn^{III}(OH_2)]^{2+}$ [4.0 mM; R = (c) NO_2, (d) Cl, (e) Me, and (f) OMe] in CD_3CN at 298 K. All spectra were recorded in CD_3CN at 298 K. The peaks marked with * in (c – f) were originated from the $dpaq^{5R}$ ligands.